Catalysis Communications 106 (2018) 60–63

Contents lists available at ScienceDirect

Catalysis Communications

journal homepage: www.elsevier.com/locate/catcom

Short communication

TiO_2 on $MoSe_2$ nanosheets as an advanced photocatalyst for hydrogen evolution in visible light

Shufang Kou, Xia Guo, Xiaofeng Xu, Jian Yang*

Key Laboratory of Colloid and Interface Chemistry, Ministry of Education, School of Chemistry and Chemical Engineering, Shandong University, Jinan 250100, PR China

ARTICLE INFO

Keywords:
Photocatalyst
Hydrogen evolution
Visible light
$MoSe_2$
TiO_2

ABSTRACT

TiO_2 grown on $MoSe_2$ nanosheets was synthesized by a simple process and explored as photocatalyst for hydrogen generation. In visible light, hydrogen generation rate over the $MoSe_2/TiO_2$ photocatalyst was found to be 468.2 μmol h^{-1} g^{-1}, much higher than the corresponding rates obtained over the $MoSe_2$, TiO_2 and their physical mixture. It is suggested that the good absorption of $MoSe_2$ to visible light and the improved charge separation by the interface of $MoSe_2/TiO_2$ greatly promote hydrogen generation rate, as supported by the transient photocurrent responses and electrochemical impedance spectra recorded.

1. Introduction

Hydrogen as one of clean energy resources has recently received intensive attention. Thus, how to generate and store hydrogen via a green, safe and cost-effective method becomes a hot topic. In various pathways, H_2 generation via photocatalysis is regarded as one of the promising ways to convert inexhaustible and pollution-free sunlight into chemical energy [1]. As early as 1970s, Fujishima and Honda realized this reaction by TiO_2 as a photoelectrode [2]. Since then, TiO_2 as a photocatalyst has been developed for various reactions, including hydrogen generation [3,4]. However, the weak light absorption to visible light and high recombination of photo-generated charges limit the performances of TiO_2 [5]. Therefore, a number of composites are being developed to address these concerns.

Recently, layer-structured transition metal dichalcogenides like MoS_2 and $MoSe_2$, have been tested as photocatalysts, due to their unique structures, narrow band gaps and weak van der Waals interactions between neighboring layers. After combined with TiO_2, the band-gap alignment between them and TiO_2 could effectively improve their performances. So far, most research works were focused on MoS_2/TiO_2, rather than $MoSe_2/TiO_2$. Tachikawa et al. [6] reported ultrathin MoS_2 shell decorated on TiO_2 mesocrystals as a photocatalyst for hydrogen evolution. Xiong et al. [7] demonstrated that metallic MoS_2 nanosheets (1T MoS_2) worked better than 2H-MoS_2 as co-catalyst of TiO_2 in photocatalysis. Zhang and Zang [8] used metal-organic frame-work (MOF) as precursor and successfully synthesized MoS_2/TiO_2. This composite, together with fluorescein as photo-sensitizer, exhibited excellent performance towards photocatalytic hydrogen generation. Compared to MoS_2, $MoSe_2$ has a higher electron conductivity [9,10]. It also has a narrow band gap of ~1.4 eV, which expands the optical absorption to the visible-light region [11]. Furthermore, $MoSe_2$ possesses a high resistance to photo-corrosion, as the optical transitions are between nonbonding metal d states [12,13]. There are only a few papers using $MoSe_2/TiO_2$ as photocatalyst. Liu and Pan [14] explored the photocatalytic performance of $MoSe_2/TiO_2$ in the photoreduction of Cr (VI). Zhu et al. [15] synthesized $MoSe_2$ nanosheets-modified TiO_2 nanowires and tested their photo-catalytic activity for degradation of methylene blue. To the best of our knowledge, the photocatalytic performance of $MoSe_2/TiO_2$ for hydrogen generation has not been explored yet.

Herein, $MoSe_2/TiO_2$ was successfully fabricated through a simple solvothermal reaction, followed by a high-temperature annealing. The photocatalytic hydrogen production rates of this composite were significantly enhanced compared to those of TiO_2 or $MoSe_2$. The improved performance of $MoSe_2/TiO_2$ could be attributed to the enhanced light absorption and high charge-separation efficiency, as supported by the obtained diffused reflection spectra (DRS), transient photocurrent response (TPR) and electrochemical impedance spectra (EIS).

2. Experimental section

Details of materials synthesis, characterization, photoelectrochemical measurements and photocatalytic tests are provided in the Supporting Information.

3. Results and discussion

Fig. 1 shows powder XRD patterns of $MoSe_2/TiO_2$ in different ratios, marked as $MoSe_2/TiO_2$-X, where X indicates the amount of tetrabutyl

* Corresponding author.
E-mail address: yangjian@sdu.edu.cn (J. Yang).

https://doi.org/10.1016/j.catcom.2017.12.013
Received 7 October 2017; Received in revised form 21 December 2017; Accepted 22 December 2017
Available online 24 December 2017

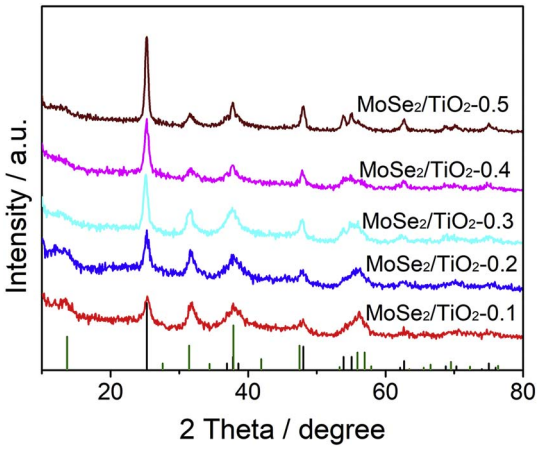

Fig. 1. Powder XRD patterns of $MoSe_2/TiO_2$-X (X = 0.1, 0.2, 0.3, 0.4 and 0.5). The bottom bars present the standard diffractograms of TiO_2 (black, JCPDS card no. 21-1272) and $MoSe_2$ (green, JCPDS card no. 29-0914). (For interpretation of the references to colour in this figure legend, the reader is referred to the web version of this article.)

titanate (TBOT) used in the synthesis. All the XRD patterns present diffraction peaks related to the $MoSe_2$ and TiO_2 crystal phases. The diffraction peaks at 25.3°, 37.9° and 48.2° are attributed to (101), (004) and (200) planes of anatase TiO_2, while those at 13.7°, 31.7°, 38.0°, 47.5° and 56.2° to (002), (100), (103), (105) and (110) faces of 2H-$MoSe_2$. These results confirm the formation of TiO_2 and $MoSe_2$ crystal phases in the composite. The wide peak widths observed indicate the small primary crystal particle sizes of TiO_2 and $MoSe_2$. As TBOT used in the synthesis procedure increases, the peak intensities of TiO_2 in the composite increase significantly, while those of $MoSe_2$ decay gradually. The presence of $MoSe_2$ and TiO_2 in the composite is also supported by Raman spectra (Fig. S1). The two peaks at 240.1 and 284.8 cm^{-1} arise from out-of-plane A_{1g} and in-plane E^1_{2g} modes of $MoSe_2$ [16,17]. The other bands at 151.0, 400.8, 516.0 and 638.4 cm^{-1} belong to the $E_g(1)$, $B_{1g}(1)$, (A_{1g} + B_{1g}), and $E_g(3)$ modes of anatase TiO_2 [18,19].

The morphology of $MoSe_2/TiO_2$-X was monitored by TEM measurements. When the hydrolysis of TBOT was conducted in the presence of $MoSe_2$ nanosheets, the small concentration and low temperature used would benefit the deposition of TiO_2 nanoparticles on $MoSe_2$ nanosheets, thus, facilitating the photo-induced charge transfer across the interface between them. As the amount of TBOT in the synthesis process increases, the continuous deposition of TiO_2 results in the encapsulation of $MoSe_2$ nanosheets by TiO_2 nanoparticles (Figs. S2–S4). The intimate contact between $MoSe_2$ and TiO_2 is directly confirmed by the HRTEM image shown in Fig. 2, where the characteristic lattice spacing at 0.660 nm from the (002) lattice planes of 2H-$MoSe_2$ and that at 0.351 nm from the (101) planes of TiO_2 could be easily observed. Similar observations were also reported in the case of MoS_2/TiO_2 [20], although there are quite differences for MoS_2 and TiO_2 in atomic arrangements and coordination environments. TiO_2 or $MoSe_2$ alone are also examined in order to understand their role in the present photocatalysis investigated, where TiO_2 appears in the form of nanoparticles (Fig. S5a) and $MoSe_2$ of nanosheets (Fig. S5b).

X-ray photoelectron spectra (XPS) were measured to disclose the valence state of elements in the surface of composite, using $MoSe_2/TiO_2$-0.3 as an example. The high-resolution spectra on Mo 3d, Se 3d, Ti 2p and O 1s were screened to give a close-up check. As shown in Fig. S6, the two peaks recorded at 228.6 eV and 231.8 eV in Mo 3d spectrum are attributed to Mo $3d_{5/2}$ and Mo $3d_{3/2}$ of Mo^{4+} in $MoSe_2$ [16,21]. The peaks recorded at 54.2 eV and 55.0 eV in Se 3d spectrum are assigned to Se $3d_{5/2}$ and Se $3d_{3/2}$ of Se^{2-} in $MoSe_2$ [16,21]. In the Ti 2p spectrum, there are two peaks centered at 458.7 eV and 464.4 eV, which are in good agreement with the characteristic peaks of Ti $2p_{3/2}$ and Ti $2p_{1/2}$ of Ti^{4+} in TiO_2 [22,23]. The O 1 s spectrum gives two peaks at 529.8 eV and 531.5 eV, where the former is related to the lattice oxygen in TiO_2 [23,24] and the latter to the Ti-OH species [22]. On the basis of these results, it can be concluded that the nanocomposite is composed of $MoSe_2$ and TiO_2, which in good agreement with the results of powder XRD, Raman and EDS.

Optical properties of $MoSe_2/TiO_2$-X were investigated by diffused reflection spectra. As depicted in Fig. S7, the absorption of TiO_2 is mainly concentrated in the region of ultraviolet light. In comparison, $MoSe_2$ shows a strong absorption band in the 300–800 nm range. Therefore, it is believed that the presence of $MoSe_2$ in the composite contributes to the absorption of visible light and TiO_2 to the absorption of ultraviolet light. In the tested composites, $MoSe_2/TiO_2$-0.3 shows the strongest absorption to visible light than the other samples of different composition in titania. This result is suggested to be due to the fact that the former material composition offers a large quantity of photo-induced electrons/holes for photocatalysis.

The efficient charge separation is another key step for photocatalysis. In order to clarify the separation efficiency of the photogenerated electron/holes, a transient photo-current was measured. The photocurrent responses of $MoSe_2/TiO_2$-X to visible light are shown in Fig. 3a. All the photocurrents of $MoSe_2/TiO_2$-X are significantly improved as compared to $MoSe_2$ and TiO_2 alone, thus confirming the fact that the combination of these two crystal phases improves the charge separation. The transient photocurrent reaches a maximum value in the case of $MoSe_2/TiO_2$-0.3. The fast charge separation could be associated with the low resistance achieved across the interface, which could be evaluated by the EIS spectra shown in Fig. 3b. Compared to the Nyquist plots of TiO_2 and $MoSe_2$, those of $MoSe_2/TiO_2$-X are fitted by a semicircle with a reduced diameter, indicating the enhanced charge-transfer kinetics. This result could be assigned to the build-in electric field at the interface of $MoSe_2$ and TiO_2, which promotes the transfer of photogenerated charges. This result is also consistent with the theoretical calculations performed on MX_2-TiO_2 (M = Mo and W; X = S and Se)

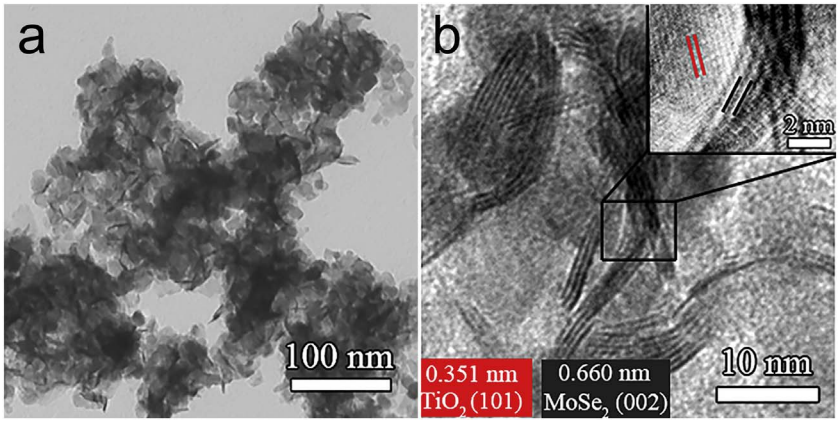

Fig. 2. (a) TEM and (b) HRTEM images of $MoSe_2/TiO_2$-0.3 solid composite.